

PHASE STABILITY OF HYDROGEN-BONDED POLYMER MIXTURES. III. SPINODAL DIAGRAMS

Julius POUCHLÝ¹, Antonín ŽIVNÝ^{2,*} and Antonín SIKORA³

*Institute of Macromolecular Chemistry, Academy of Sciences of the Czech Republic,
162 06 Prague 6, Czech Republic; e-mail: ¹ pouchly@imc.cas.cz, ² zivny@imc.cas.cz,
³ sikora@imc.cas.cz*

Received June 1, 1998

Accepted July 8, 1998

Dedicated to the memory of Professor Otto Wichterle.

Relations derived on the basis of the Barker–Guggenheim quasichemical theory were used for construction of spinodal diagrams (temperature *versus* composition) of a mixture of two polymers in which hydrogen bonds and other strong interactions exist. A function dependence of parameters of quasichemical equilibrium, η , was proposed, which has the form of the Boltzmann function at lower temperatures, but at higher temperatures corresponds to random mixing. The spinodal diagrams were constructed for several sets of dependences of η on temperature in a wide temperature range for different chain lengths, r , or for different values of the content of polar groups in one of the polymers. According to circumstances, the phase diagram shows one or two temperature regions of phase instability or the phase instability occurs in a certain range of composition at any temperature. Though the chain length was chosen equal for both polymers, the phase diagrams are asymmetric in the sense that the critical points are shifted towards that border of the diagram which corresponds to the component with a larger relative content of the polar group. The temperature range of phase instability is strongly influenced by small changes in the relative surface area of polar groups in the molecules.

Key words: Polymer mixtures; Hydrogen bonds; Quasichemical equilibrium theory; Spinodal diagrams; Critical solution temperature.

A great variety of different types of interactions occur in a mixture of two polymers containing both polar groups and nonpolar residues. The miscibility of the polymers is enhanced by formation of hydrogen bonds or another type of strong interaction between them; the other interactions may sometimes lead to limited miscibility even in the case of formation of a strong interassociation complex (see the preceding communication).

Spinodal curves, *i.e.*, border lines between regions of phase metastability and instability in the diagram temperature–composition, may acquire very

different forms in systems with more types of interaction. Coleman and Painter (see, *e.g.* refs^{1,2}) calculated model phase diagrams on the basis of the theory of association equilibria, *i.e.*, under the assumption of chemical equilibrium of species formed by an action of hydrogen bonds. In our previous communications^{3,4}, we have shown that a good alternative to the mentioned theory is the Barker–Guggenheim theory of quasichemical equilibrium because it describes the influence of all types of contact interactions equally well. We have made calculations of the second derivative of the Gibbs energy of mixing with respect to composition for a mixture of polymer component 1 containing polar groups A with polymer component 2 containing polar groups B while both polymers have a nonpolar rest R of the same chemical nature. In literature³, general relations were derived and the effect of non-random mixing on thermodynamic behaviour was analyzed. In literature⁴, we dealt with systems characterized by strong preference for heterocontacts AB, AR and BR and we analyzed the condition of phase instability at a given temperature. It followed that the phase separation originates in a difference in relative contents of polar groups in molecules of 1 and 2. This is also supported by small values of constants η of the quasichemical equilibrium expressing the thermodynamic affinity to formation of heterocontacts. In this paper, we extend our calculations to a wide range of temperatures, which involves a continuous transition from large to small deviations from random mixing, and we discuss spinodal diagrams temperature–composition for several types of systems. The parameters of the quasichemical equilibria, η_{AB} , η_{AR} and η_{BR} are expressed as functions of temperature using entropic constants λ and enthalpic parameters ε . In each phase diagram, parameters η thus change from very small or very large values characteristic of low temperatures to values not far from unity (random mixing) at higher temperatures. The calculations were made for several sets of values of λ and ε and evolution of spinodals with increasing length of polymer chains and/or increasing difference in the content of polar groups A and B in corresponding polymers was followed.

THEORETICAL

The spinodal curve satisfies the condition

$$\left(\partial^2 \Delta G_N / \partial \phi_1^2\right)_{T,P} = 0 \quad (1)$$

at any temperature. (For symbols not explained here, see the paragraph Basic Equations in our preceding paper⁴). The second derivative of Gibbs energy

with respect to composition can be obtained using relations and definitions given in Eqs (1) through (18) in our previous paper⁴. In addition, we have to define functions which assign values of η_{KL} to a given temperature, η_{KL} being the equilibrium constant for a process of formation of an interaction contact of unlike groups K and L at the expense of contacts of like groups (KK and LL); cf. Eq. (1), ref.⁴. We start from the following assumptions:

1. The parameter η_{KL} can be expressed as the ratio of partition functions of participating pairs

$$\eta_{KL}^2 = \frac{q_{KL}^2}{q_{KK} q_{LL}} . \quad (2)$$

2. Partition functions for A-R, B-R and R-R pairs in which at least one nonpolar group participates have insignificant temperature dependence so that it can be neglected in comparison with pairs named sub 3.

3. Partition functions for pairs of polar groups A-A, B-B and A-B show strong temperature dependence at low temperatures determined by bonding energies of pairs. However, in the range of high temperatures, due to thermal disorientation of groups, the temperature dependence is equally negligible like with pairs mentioned sub 2 and for very high temperatures, the condition of random mixing should be fulfilled

$$\lim (T \rightarrow \infty) \eta_{KL} = 1 . \quad (3)$$

The simplest functional form fulfilling the assumptions just mentioned is for η_{AR} and η_{BR} given by the equation

$$\eta_{KR} = [1 + \lambda_{KK} \exp(-\varepsilon_{KK} / RT)]^{-1} \quad (K \equiv A; B) . \quad (4)$$

The presence of parameters λ_{AA} and ε_{AA} in the equation for η_{AR} follows from assumptions 1 through 3. Under the same assumptions, we obtain for η_{AB} the equation

$$\eta_{AB} = \frac{[1 + \lambda_{AB} \exp(-\varepsilon_{AB} / RT)]^2}{[1 + \lambda_{AA} \exp(-\varepsilon_{AA} / RT)][1 + \lambda_{BB} \exp(-\varepsilon_{BB} / RT)]} , \quad (5)$$

$\lambda_{KL} > 0$, $\varepsilon_{KL} < 0$ holds in the above equations. η_{AR} and η_{BR} parameters thus acquire very small values at low temperatures and with increasing temperature, they approach asymptotically $(1 + \lambda_{AA})^{-1}$ and $(1 + \lambda_{BB})^{-1}$, respectively. Constants λ reflect a local decrease in entropy due to mutual orientation of two interacting groups and are then substantially smaller than unity; so, the condition (3) is satisfied to a good approximation. The temperature dependence of η_{AB} may be more complex. At low temperatures, the η_{AB} parameter can reach very high or very low values depending on the sign of the difference $\Delta\varepsilon_{AB}$:

$$\lim(T \rightarrow 0) \ln \eta_{AB} \cong -\Delta\varepsilon_{AB} / RT, \quad (6)$$

$$\Delta\varepsilon_{AB} = 2\varepsilon_{AB} - (\varepsilon_{AA} + \varepsilon_{BB}) . \quad (7)$$

At intermediate and higher temperatures, it is a matter of proportions of λ_{AA} , λ_{BB} and λ_{AB} values whether the $\eta_{AB}(T)$ dependence will have a monotonous course or the sign of the difference $\eta_{AB} - 1$ will be changed at some temperature and, consequently, an extreme on the curve appears. From these temperature dependences of η parameters, the enthalpy of formation of A-R contacts at the expense of A-A and R-R contacts follows:

$$h_{AR} = -(1 - \eta_{AR}) \varepsilon_{AA} , \quad (8)$$

where h_{AR} is related to one mole of A-R contacts. An analogous relation is valid for B-R contacts. The enthalpy of A-B contacts is given by the relation

$$h_{AB} = -(1 - \eta_{AR}) \varepsilon_{AA} - (1 - \eta_{BR}) \varepsilon_{BB} + 2(1 - \eta_{ABR}) \varepsilon_{AB} , \quad (9)$$

where the η_{ABR} parameter, pertinent to the quasichemical equilibrium



is temperature-dependent according to equation

$$\eta_{ABR} = [1 + \lambda_{AB} \exp(-\varepsilon_{AB} / RT)]^{-1} . \quad (11)$$

The contact enthalpy then depends on temperature due to disorientation of interacting groups by thermal motion (assumption 3). In the limit for low temperature, where $\eta_{KR} \rightarrow 0$, we obtain

$$h_{KR} = -\varepsilon_{KK} \quad (K \equiv A; B) , \quad (12)$$

$$h_{AB} = \Delta\varepsilon_{AB} . \quad (13)$$

RESULTS

For model calculations of spinodal diagrams, we have chosen sets of λ and ε values given in Table I. The set of parameters Ic was derived from the set Ia by exchange of subscripts A for B (and *vice versa*). In the set Ib, the values $\lambda_{AA} = \lambda_{BB}$ were calculated as geometrical means of λ_{AA} and λ_{BB} values in the set Ia; parameters $\varepsilon_{AA} = \varepsilon_{BB}$ are arithmetic means of parameters ε_{AA} and ε_{BB} chosen for the set Ia. Consequently, in systems with parameters Ib, $\eta_{AR} = \eta_{BR}$ at any temperature.

For each of the (λ , ε) sets, parameters α_A , α_B , r_1 and r_2 need to be specified. Here, α_A is the relative area of contact sites of type A in a molecule of component 1, and α_B is related to B sites in a component 2 molecule; r_j stands

TABLE I
Parameters of the temperature dependence of quasi-equilibrium constants

Set	λ_{AA}	λ_{BB}	λ_{AB}	$-\varepsilon_{AA}, \text{ J mol}^{-1}$	$-\varepsilon_{BB}, \text{ J mol}^{-1}$	$-\varepsilon_{AB}, \text{ J mol}^{-1}$
Ia	0.05477	0.1465	0.07422	13 282	9 818	13 251
Ib	0.08958	0.08958	0.07422	11 550	11 550	13 251
Ic	0.1465	0.05477	0.07422	9 818	13 282	13 251
II	0.00248	1.39×10^{-4}	0.00158	19 031	25 034	20 903

for the number of segments in a molecule of component j . We have put $r_1 = r_2 = r$ and investigated the effect of r and of $(\alpha_A - \alpha_B)$ on the course of phase diagrams.

In order to present as many shapes of spinodals as possible, we have used a wide range of temperatures from the lowest values up to 600 K. A real system may thus correspond only to some sector of our diagrams. On the other hand, the predicted shapes of spinodals are not confined to temperature ranges occurring in our diagrams. The phase diagram (or its part), which originally involves the temperature range from T_1^0 to T_2^0 , could be transposed in a qualitatively similar form to the range from T_1 to T_2 by transformation of constants ε_{KL}^0 and λ_{KL}^0 into constants ε_{KL} and λ_{KL} ($K; L \equiv A; B$)

$$\varepsilon_{KL} = \varepsilon_{KL}^0 \frac{1/T_2^0 - 1/T_1^0}{1/T_2 - 1/T_1}, \quad (15)$$

$$\lambda_{KL} = \lambda_{KL}^0 \exp\left(\frac{\varepsilon_{KL}^0}{R} \frac{T_2/T_2^0 - T_1/T_1^0}{T_1 - T_2}\right). \quad (16)$$

The results of our spinodal calculations will be presented in two parts: In the first one we use the sets of parameters Ia, Ib and Ic from Table I, the results obtained for the set II will be given in the second part. The titles of the two parts involve the important difference in the course of temperature dependence of η_{AB} , but there are also differences in the mutual positions of the three $\eta(T)$ curves.

Monotonous Change of Equilibrium Parameters with Temperature

The temperature dependences of parameters $1/\eta_{AB}$, η_{AR} and η_{BR} for systems of the set Ia are depicted in Fig. 1. With increasing temperature, η_{AB} monotonously decreases from very high values to values close to unity; however, in the entire temperature range, η_{AB} is smaller than η_{AR}^{-1} or η_{BR}^{-1} . The diagram for the set Ic can be obtained from Fig. 1 by the interchange of curves for η_{AR} and η_{BR} ; the common curve $\eta_{AR} = \eta_{BR}$ for the system Ib is located approximately in the middle between the curves in Fig. 1. For the system Ia at temperatures higher than 420 K (but for the system Ic at $T < 420$ K), $\eta_{AR} > \eta_{BR}$.

In this temperature range, the polar group A (with larger relative area) shows greater affinity to the formation of contacts with the nonpolar group R than the group B. This improves somewhat miscibility of both components in comparison with the system Ib. The opposite conclusion holds for

the complementary range of temperatures ($T < 420$ K for Ia; $T > 420$ K for Ic). At low temperatures (up to 200 K), we have the case of a polymer-polymer complex with a simultaneous repulsive interaction of polar and nonpolar groups; this is just the type of systems we have dealt with in the previous paper.

The change in the shape of spinodal diagrams with increasing chain length is depicted in Fig. 2. A high-temperature region of phase instability appears even at low values of r and its lower critical solution temperature (LCST) gradually decreases. At $r = 550$, a closed region of phase instability appears in the vicinity of 220 K, which quickly extends toward lower temperatures until its LCST disappears. The lower part of this region (below 100 K) is limited by vertical spinodal branches as it was predicted in the previous paper for small values of $1/\eta_{AB}$, η_{AR} and η_{BR} on the basis of a negligible temperature dependence of the quantity Z ; cf. Eq. (36) and the ensuing analysis in ref.⁴. However, in the vicinity of 100 K, the spinodal changes its slope and the region of phase instability somewhat widens. This can be explained on the basis of Eq. (37) of the previous paper⁴. At a given temperature, both spinodal points ($Z = 0$) differ only very little in their compositions ϕ_1 and the slope ($\partial Z / \partial \phi_1$) is then very small. That is why even a small increase in the derivative $(\partial Z / \partial T)_{\phi_1}$ in the vicinity of 100 K is sufficient for a significant change in the spinodal slope.

The upper critical solution temperature (UCST) of the low-temperature region gradually increases with increasing chain length; if r approaches

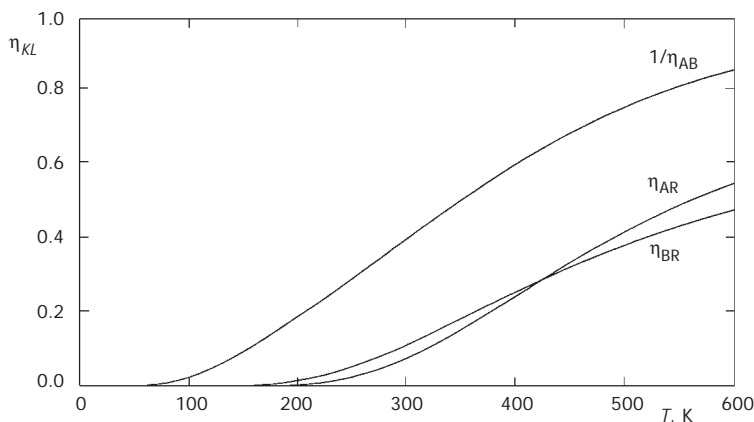


FIG. 1

Dependence of parameters of the contact equilibria, $1/\eta_{AB}$, η_{AR} and η_{BR} , on temperature for systems of set Ia (for constants λ and ε , see Table I)

800, the UCST approaches the LCST of the high-temperature region so that at $r \cong 793$, both regions coincide to form a continuous region of the phase instability. This region widens with increasing r .

The described evolution is summarized in Fig. 3 presenting the dependence of the critical solution temperature on the chain length. The curve has several branches corresponding successively to the LCST of the high-temperature region, and to the UCST and LCST of the low-temperature region. The region of the phase instability lies to the right of the boundary curve. The behavior of sets Ib and Ic is also depicted in the same figure. The curves intersect in one point corresponding to critical temperature 420 K and to $r = 770$. This point corresponds to the intersection of curves $\eta_{AR}(T)$ and $\eta_{BR}(T)$, which occurs in sets Ia and Ic at the latter temperature. In the region below 420 K, the system Ia is the least miscible and the system Ic is the most miscible due to the validity of inequality $\alpha_A > \alpha_B$. That is why the merging of the high-temperature with the low-temperature instability region already occurs in the system set Ia at $r \cong 793$, in the set Ib at $r \cong 1\ 800$ and in the case of the set of systems Ic not until at $r \cong 11\ 800$. On the other hand, the systems of set Ic show the greatest tendency to phase segregation at temperatures above 420 K.

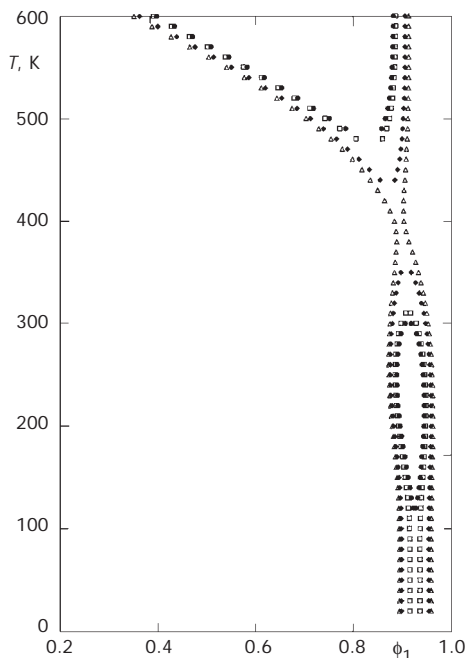


FIG. 2
Spinodal diagrams (temperature versus composition) for systems of set Ia (for constants λ and ε , see Table I) differing in the chain length r ($r = r_1 = r_2$), $\alpha_A = 0.25$; $\alpha_B = 0.10$; ● $r = 630$; □ $r = 650$; ◆ $r = 750$; △ $r = 800$

Equilibrium Parameter $\eta_{AB}(T)$ Showing a Maximum

The systems belonging to series II have the temperature dependence of η parameters substantially different from that in series I. We can see from Fig. 4 that η_{AB} is smaller than unity at very low temperatures; the affinity to the complex formation increases with increasing temperature so that η_{AB} attains its maximum value 2.5 at 285 K and then gradually decreases toward values close to unity. In comparison with the series I, the parameter attains substantially lower values. The constant η_{AR} is smaller than η_{BR} at temperatures above 250 K ; with a positive difference $\alpha_A - \alpha_B$, this leads to a decrease in miscibility; however, this factor is overcompensated by the fact that both the η_{AR} and η_{BR} values are significantly higher than those in series I. The spinodal diagrams of series II also show in many respects a different temperature dependence of phase instability than in the previous series, as is obvious from Fig. 5. The low-temperature region of phase instability, substantiated by a low value of η_{AB} , already appears with short chains, and its UCST gradually increases with increasing r until it merges with the LCST of the high-temperature region. In the range of higher temperatures, a closed immiscibility region appears at $r = 310$ and $T \cong 450$ K, growing with increasing r more quickly towards higher than towards lower temperatures. Nevertheless, merging with the low-temperature region occurs at $r = 1\ 950$

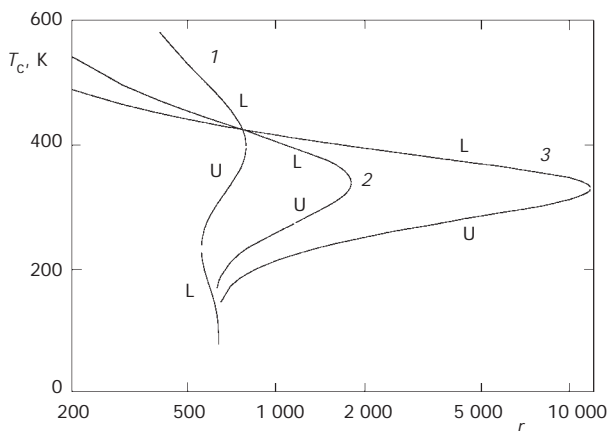


FIG. 3

Dependence of the critical solution temperature T_c on the chain length r . Curves: 1 set Ia; 2 set Ib; 3 set Ic (for parameters, see Table I); L lower critical solution temperature, U upper critical solution temperature

and $T = 320$ K. In contrast to systems of series I, both instability regions in series II assume a substantially wider range of ϕ_1 . The described changes in the critical temperatures with increasing chain length are presented in

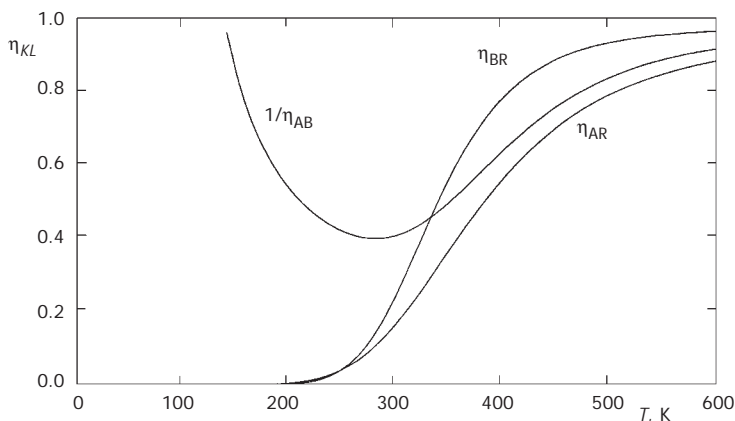


FIG. 4

Dependence of parameters of the contact equilibria, $1/\eta_{AB}$, η_{AR} and η_{BR} , on temperature for systems of set II (for constants λ and ε , see Table I)

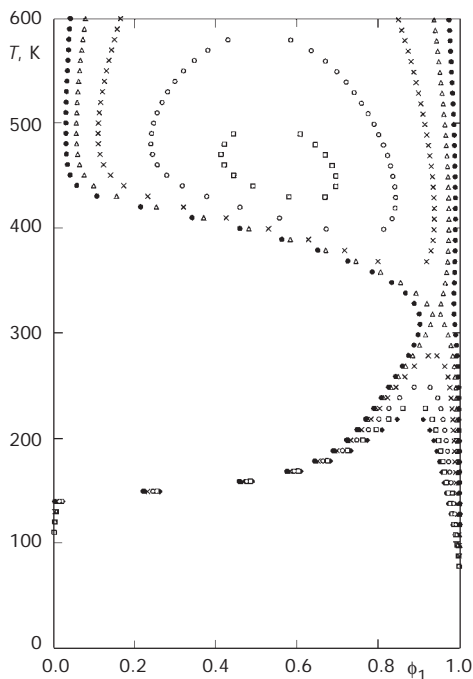


FIG. 5

Spinodal diagrams (temperature versus composition) for systems of set II (for constants λ and ε , see Table I) differing in the chain length r ($r = r_1 = r_2$), $\alpha_A = 0.25$; $\alpha_B = 0.10$; \blacklozenge $r = 300$; \square $r = 350$; \circ $r = 500$; \times $r = 1000$; \triangle $r = 2000$; \square $r = 4000$

Fig. 6. In addition, the dependence on the content of polar groups B at constant r and α_A is shown in the same graph. This dependence of T_c on α_B has the opposite slope than the dependence of T_c on r and the phase-unstable systems lie to the left of curve 2. It is clear from the graph that phase behaviour is very sensitive to small changes in the surface area of polar groups; while in the case of curve 1, its branches merge at $r = 310$ and $r = 1\,950$ (LCST is thus within $\Delta r = 1\,640$), in the case of curve 2, we observe the same effect in the range of α_B from 0.108 to 0.093 (corresponding to $\Delta\alpha_B = 0.015$). A similar conclusion is valid in the case of systems of series I. Another example of the effectiveness of small changes in parameter α_B is given in Fig. 7. Curve 1 is the limit of the curve sequence in Fig. 5 for very long chains. The region of phase instability is continuous in the entire temperature range and, owing to great values of r , embraces a wide range of compositions ϕ_1 . It is clear from curve 2 that a small decrease in the difference $\alpha_A - \alpha_B$ splits the instability region into two zones separated by a miscibility window, and this holds even for very long chains.

DISCUSSION

The systems of series I and II have a common feature: in a certain range of r , two temperature regions of phase instability appear which approach each

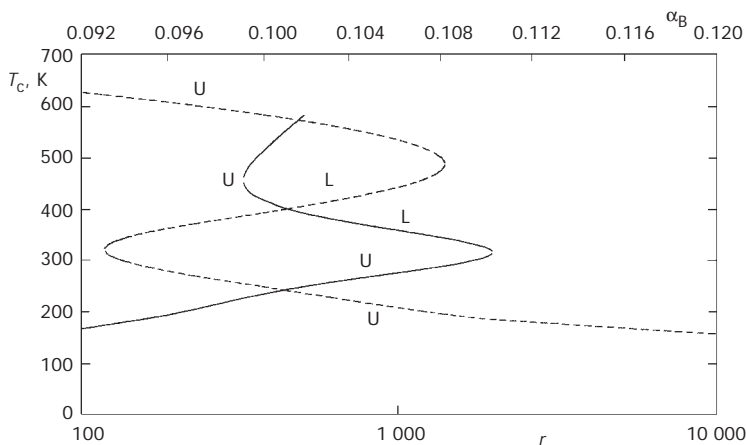


FIG. 6

Dependence of the critical solution temperature, T_c , in systems of set II (see Table I) on the chain length r (full line, $\alpha_A = 0.25$; $\alpha_B = 0.10$) and on the relative content of contact sites of type B, α_B (dashed line, $\alpha_A = 0.25$, $r = 500$); L lower critical solution temperature, U upper critical solution temperature

other with increasing r . Finally, they can merge so that they cover the whole temperature range studied. Both series differ significantly in the form of their spinodals.

A significant feature of the phase diagrams displayed is their asymmetry with respect to the axis $\phi_1 = 0.5$: critical points (and often the whole instability region) are strongly shifted towards the border value $\phi_1 = 1$ regardless of the fact that both kinds of chains contain equal numbers of segments ($r_1 = r_2$). In a classical Flory-Huggins system with constant χ parameter, the asymmetry can occur just at a significant difference in chain lengths. In our model systems, the essential factor is non-random mixing (*i.e.*, η parameters different from unity); however, it can only result in asymmetry if the components differ in their relative contents of polar groups ($\alpha_A > \alpha_B$). The maximum of Z lies in the vicinity of the "point of equivalence" where $\psi_A = \psi_B$ holds. This point corresponds to the composition

$$\theta_1 = \alpha_B / (\alpha_A + \alpha_B) \text{ and } \theta_2 = \alpha_A / (\alpha_A + \alpha_B) ,$$

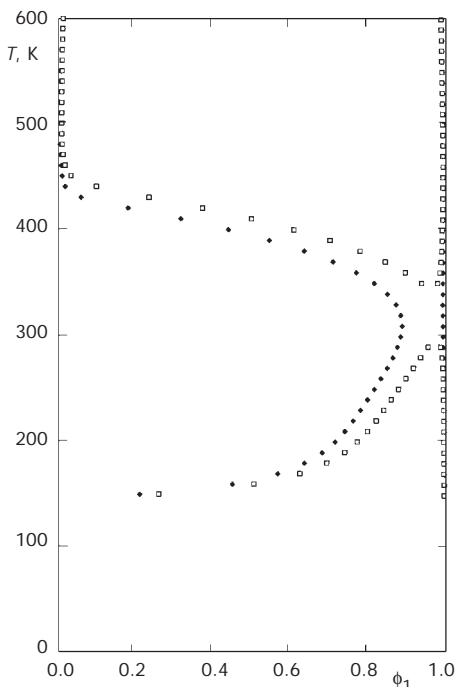


FIG. 7

Spinodal diagrams (temperature *versus* composition) for systems of set II (see Table I) with very long chains differing in values of α_B ($\alpha_A = 0.25$). Curves: \blacklozenge $\alpha_B = 0.1$; \square $\alpha_B = 0.105$

at which the component with lower value of α prevails (in our case, $\theta_1 < 0.5$). The instability region ($Z < 0$) is then situated in the opposite half of the phase diagram (see curve 4 in Fig. 3 of ref.⁴), *i.e.*, in the region where the lack of the minority polar groups is especially great.

The asymmetry of the spinodal curve is greater with increasing values of parameters η_{AR} , η_{BR} and $1/\eta_{AB}$; it is then the greatest in the low-temperature regions of instability in systems of type I. On the other hand, the UCST of the high-temperature region in systems of series II lies in the vicinity of $\phi_1 = 0.5$ because all three η constants already approach unity in the neighbourhood of $T = 600$ K.

Indeed, strict application of the theory of quasicheical equilibria assumes that in any system at sufficiently high temperatures, all η parameters approach the value of unity characteristic of random mixing. Consequently, phase stability occurs. Corresponding to this, an upper critical point can be seen for short-chain mixtures in Fig. 5; for long chains, it may be expected at higher temperatures. However, the Barker–Guggenheim theory does not include the influence of difference in the thermal expansivity of both components which is described by the equation-of-state theory^{5,6}. As it is known, such a difference leads to a limitation of miscibility which increases with increasing temperature. The miscibility behaviour in this temperature range could be described by a theory involving the two effects, which would result in a prohibitively complex algorithm.

The authors wish to thank the ČS-US scientific technical program (grant No. 950024) and the Grant Agency of the Academy of Sciences of the Czech Republic (grant No. A4050605) for financial support of this work.

REFERENCES

1. Coleman M. M., Graf J. F., Painter P. C.: *Specific Interactions and the Miscibility of Polymer Blends*. Technomic Publishing, Lancaster 1991.
2. Coleman M. M., Painter P. C.: *Prog. Polym. Sci.* **1995**, 20, 1.
3. Pouchlý J., Živný A., Sikora A.: *Collect. Czech. Chem. Commun.* **1995**, 60, 1830.
4. Pouchlý J., Živný A., Sikora A.: *Collect. Czech. Chem. Commun.* **1999**, 64, 13.
5. Patterson D.: *Macromolecules* **1969**, 2, 672.
6. Siow K. S., Delmas G., Patterson D.: *Macromolecules* **1972**, 5, 29.